TABLE 1 Complex Permittivity Values of PBT Obtained by Two Different Methods

	Small Perturbation Method	FP Approach
ε'	3.27 ± 0.24	3.07 ± 0.16
ε''	0.102 ± 0.023	0.116 ± 0.019

For characterization of the samples, a measurement frequency around 12.8 GHz (between 12.64 and 13.10 GHz) was used. The measurements were performed five times in order to obtain a complex permittivity mean value. At the center of the cavity, we have a hole that corresponds to the maximum electric-field position, in which a PTFE sampler holder is inserted. For the initial calibration, we used a rodlike sample of PTFE, which is substituted latter by an identical sample of polybutylene terephtalate (PBT). Figure 2 shows the amplitude response of the cavity with the empty sampler holder and the PBT sample.

The achieved cavity response (amplitude and phase) was adjusted to the response by Eq. 1, using a Nelder–Mead unconstrained nonlinear minimization algorithm. The introduction of the sample results in a change of the cavity refractive index, which is proportional to the sample volume and geometry. This proportional constant is obtained using a calibration sampler (PTFE). Figure 3 displays the experimental cavity response and the simulated one after the minimization process. After the minimization process we obtain 3.07 and 0.116 for the real and imaginary parts of the dielectric permittivity, respectively. To evaluate the precision of our method, we apply the small-perturbation technique to the same measured values [5]. In Table 1, we compare the measured values for the complex permittivity when applying both techniques.

4. CONCLUSION

We have proposed an innovative technique to measure the complex permittivity of samples, based on the frequency response of resonant cavities. The cavity response was adjusted to the transfer function of a Fabry–Perot filter, and good agreement between then was obtained. The values obtained for the permittivity of a PBT sample were compared to the ones obtained for the same sample using the small-perturbation theory, in order to check the accuracy of the measurement.

ACKNOWLEDGMENTS

This work was supported by the POSI program, which is financed by the European Union FEDER fund and the Portuguese scientific program. We thank Teka and Quiminova for the synthesis of the polymeric material used in this work.

REFERENCES

1. C.M. Weil, C.A. Jones, Y. Kantor, and J.H. Grosvenor, On RF material characterization in the stripline cavity, IEEE Trans Microwave Theory Tech 48 (2000), 266–275.
2. A. Kraszewski and S.O. Nelson, J Microwave Power Electron Ener 31 (1996), 178–187.
3. F. Henry, Développement de la métrologie hyperfréquences et application a l'étude de l'hydratation et la diffusion de l'eau dans les matériaux macromoléculaires, Ph.D. thesis, Paris, 1982.
4. C. Heutschel, Fabry–Perot interferometer, Fiber optics handbook, 3rd ed., Hewlett Packard, 1989.
5. L.C. Costa, S. Devesa, and P. André, Microwave dielectric proprieties of glass reinforced polymers, Material Research Innovations, 2004.

ANTENNA-BEAM SHAPING FROM OFFSET DEFECTS IN UC-EBG CAVITIES

Y. Hao, A. H. Alomainy, and C. G. Parini
Department of Electronic Engineering
Queen Mary, University of London
London E1 4NS, U.K.

Received 23 March 2004

ABSTRACT: *We present a new application of uniplanar compact electromagnetic bandgap (UC-EBG) structures in antenna-beam shaping for indoor mobile communications. Such UC-EBGs are used to construct Fabry–Perot-type cavities in which the enhanced directivity can be achieved from conventional patch antennas. This paper demonstrates that an antenna beam can be shaped by shifting the defects (patch antennas) from the centre of UC-PBG cavities. The theoretical predictions are verified by numerical simulations and measurement results, and it appears that antenna-beam shaping in UC-EBG cavities can achieve the same radiation patterns as complex planar-antenna arrays used for improving the quality and strength of sent/received signals in mobile base stations.* © 2004 Wiley Periodicals, Inc. Microwave Opt Technol Lett 43: 108–112, 2004; Published online in Wiley InterScience (www.interscience.wiley.com). DOI 10.1002/mop.20391

Key words: *electromagnetic band gap (EBG); Fabry–Perot cavities; microstrip antenna; shaped beam pattern*

1. INTRODUCTION

Electromagnetic band gap (EBG) structures, also called photonic band gap (PBG) structures [1, 2], offer pass- and stop-bands to electromagnetic waves in the same way semiconductors offer these properties to electrons. Its application to antennas and RF passive components includes the suppression of surface waves [3, 4] the construction of Perfect Magnetic Conducting (PMC) planes [5], antenna-gain improvement [6], isolation enhancement in the diplexer [7] and self-diplexing patch antennas [8], and so forth. It is also noted in [9, 10] that high directivity can be obtained from conventional patch antennas using a defect mode of Fabry–Perot-type EBG cavities in the same way as photonic devices in PBGs [12, 13]. Most of the directive photonic antennas are constructed from either layered dielectric materials with different permittivity (commonly called Bragg mirrors) or alumina rods layers and thin cylindrical metal wires [9–13]. Under this circumstance, Bragg reflections are achieved with a one-dimensional (1D) EBG/PBG, and hence the enhanced directivity is limited. By extending the periodicity from one to two dimensions, it is possible to control the electromagnetic-wave propagation in a plane and therefore achieve a pencil-like radiation beam from single radiators, such as monopole or patch antennas. This technique was verified recently by Sauleau [14] using plane-parallel nonuniform metallic-strip gratings as reflecting mirrors in order to achieve Gaussian-beamlike directive antennas.

We present below a new directive antenna design using uniplanar compact (UC) EBG structures as Fabry–Perot cavities. UC-EBG [3, 15] has the advantage of ease of fabrication, and most UC-EBGs have been made by etching a class of periodic patterns on the metallic ground plane. Furthermore, our studies demonstrate that one can obtain a shaped antenna beam by simply shifting radiators from the centre in the proposed UC-EBG cavities. In this paper, the properties of the proposed Fabry–Perot cavities made from single-layer and double-layer UC-EBGs, respectively, are examined. Specifically, the radiation characteristics from the offset defects in the cavity are investigated as compared

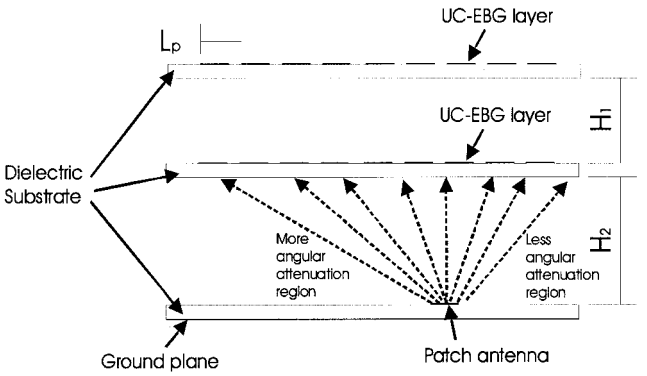

Figure 1 Side view of the layered UC-EBG cavity proposed for antenna-beam shaping

with those from the offset defects in the centre. Experimental verification has been made using a conventional microstrip-patch antenna as the defect in the cavity. Such antennas demonstrate the improved radiation properties with high directivity, and the evidence of beam shaping is also demonstrated. For the demonstration, all designs are made at 5.15–5.35 GHz for HiperLAN applications and the simulation results are presented with experimental verification.

2. THEORY AND DESIGN

Naturally occurring electromagnetic fields can be represented by the superposition of either a discrete set or a continuum of plane waves travelling in different directions. Such a set of plane waves is known as an angular spectrum [16]. For many microwave antennas, the angular spectrum is of negligible amplitude outside a narrow range of angles. When such antennas are placed inside Fabry–Perot-type EBG cavities, the latter acts as spatial filters, which only let a certain amount of angular spectral components pass and thus focus the incident fields radiating from the antennas [14].

The geometry of a layered UC-EBG cavity used in this paper for antenna-beam shaping is shown in Figure 1, and the structure consists of UC-EBGs as angular filters with a conventional patch antenna as radiating source. UC-EBGs and the metallic ground plane form a Fabry–Perot-type cavity and the patch antenna is seen as a defect in the cavity. Reference [9] indicates that the distance from the patch antenna to the UC-EBG is set to be a half-wavelength at the resonating frequency in order to maximize the power radiating from the source. However, considering the perturbation from thin dielectric substrates, according to our experience, the distance H_2 should be optimized as 30 mm at 5.2 GHz. The cavity design is completed by using an additional UC-EBG layer to enhance its reflectivity. The distance between two EBG layers H_1 is set as $\lambda_o/4$ at the operating frequency. The main interest in having two UC-EBG layers is that they can be used to construct a dielectric mirror, also known as a Bragg reflector, which consists of identical alternating layers of high and low refractive indices. The standard arrangement is to have an odd number of layers, with the high-index layer being the first and last layer. However, since the quarter-wave layers are present, such a UC-EBG cavity acts as a narrow transmission filter, with the transmission bandwidth becoming narrower as the number of layers increases.

In applications like WLANs, the limited available power from access points must be evenly distributed over wide areas, without creating over- or underilluminated zones. This implies that the antenna's radiation pattern must compensate for path loss, which corresponds to the well-known cosec^2 characteristic in the elevation plane. The antennas are also required to discriminate multipath losses by diversity, and hence sector coverage in the azimuth plane is required. Conventionally, such antennas can be made from linear arrays arranged in pyramid shape [17], with the shaped antenna beam achieved by complicated feeding networks that bring extra costs and losses to the system. The idea of using the EBG cavity to shape the antenna beam is very straightforward. Once the defect (namely, the patch antenna) in the cavity is offset from the centre, its angular spectrum of radiation field will be alternated and become asymmetrical due to uneven attenuation from the EBG (Fig. 1); indeed, antenna-beam shaping can be further designated by changing EBG patterns.

3. UC-EBG CAVITIES AND ANTENNAS

Figure 2 show photographs of the proposed UC-EBG cavity antennas. Both the UC-EBG and the patch antenna were fabricated on RT/Duroid boards with substrate thickness 1.524 mm and dielectric constant 3. The periodicity of the UC-EBG structure is given by

$$l_p \approx \frac{\lambda_g}{2} = \frac{c}{2\sqrt{\varepsilon_{eff} f_{res}}}, \tag{1}$$

where λ_g is the guided wavelength at the operating frequency f_{res}, c is the speed of light in free space, and ε_{eff} is effective permittivity. This produces an approximated period of 20 mm at 5.2 GHz.

The proposed UC-EBG structure was analysed to examine the band-gap characteristics at different incident angles of electromagnetic waves. Figure 3 shows frequency response obtained using Agilent Momentum™ and exhibits distinct band gaps in its transmission response of the UC-EBG structure at different angles of wave incidence. The dimensions of the rectangular patch are 16.30 × 12.74 mm. The 50Ω line width is 3.9 mm. The width and length of the impedance transformers are 0.4 and 8.3 mm, respectively. The measured resonant frequency is shown in Figure 4 at 5.09 GHz and is in good agreement with the simulation. Its E-plane radiation pattern is shown in Figure 5. When the patch antenna is placed in the UC-EBG cavity, antenna-beam narrowing is evident from the measurement results (Fig. 5), even when only a one-layer UC-EBG is used. The simulated antenna directivity is improved from 6 to 20 dB and the main beamwidth was narrowed by approximately 60%, in comparison with the pattern of the conventional patch antenna. The cross-polar patterns present a low level of radiation, which implies a low level of backward radiation. When two EBG layers are used in the cavity, the antenna directivity increased to 22 dB with a beamwidth of less than 25° (Fig.

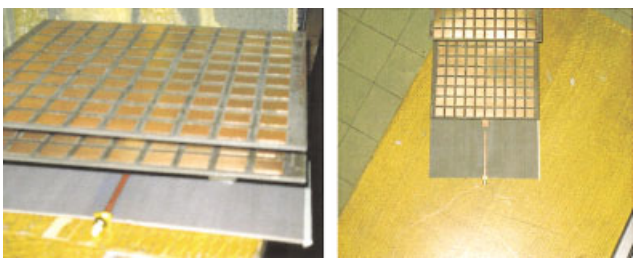

Figure 2 Photographs of the microstrip antenna embedded within the cavity bounded by the ground plane and the EBG structure. [Color figure can be viewed in the online issue, which is available at www.interscience.wiley.com.]

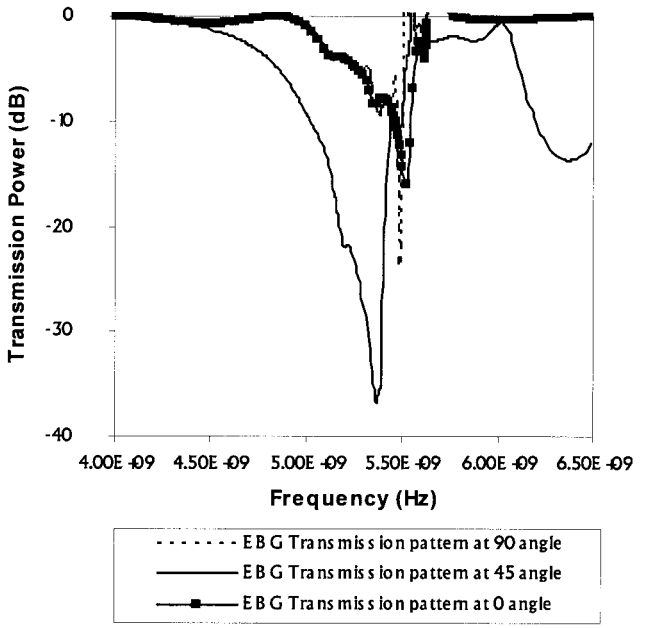

Figure 3 Simulated UC-EBG frequency responses at different wave-incidence angles (simulation performed using Agilent ADS/Momentum)

5). Both simulated and measured antenna return losses are shown in Figure 4.

The radiation-pattern measurements of the UC-EBG cavity antenna (with two EBG layers) produced added improvements in directivity and beamwidth of the main lobe and are in good agreement with simulation results (Fig. 6). The differences in the side-lobe levels between the measured and simulated patterns are due to the assumption of an infinite ground plane, considered in the Agilent Momentum™ simulation package.

4. BEAM-SHAPING ANALYSIS AND RESULTS

As our main objective for the work presented here is to introduce the property of beam shaping of a radiation pattern by applying

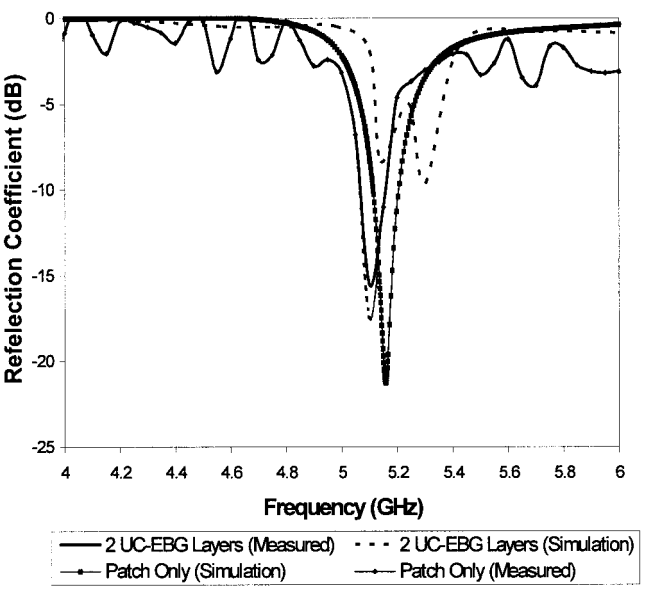

Figure 4 Comparison of simulated and measured return-loss responses for both cases with/without UC-EBG layers

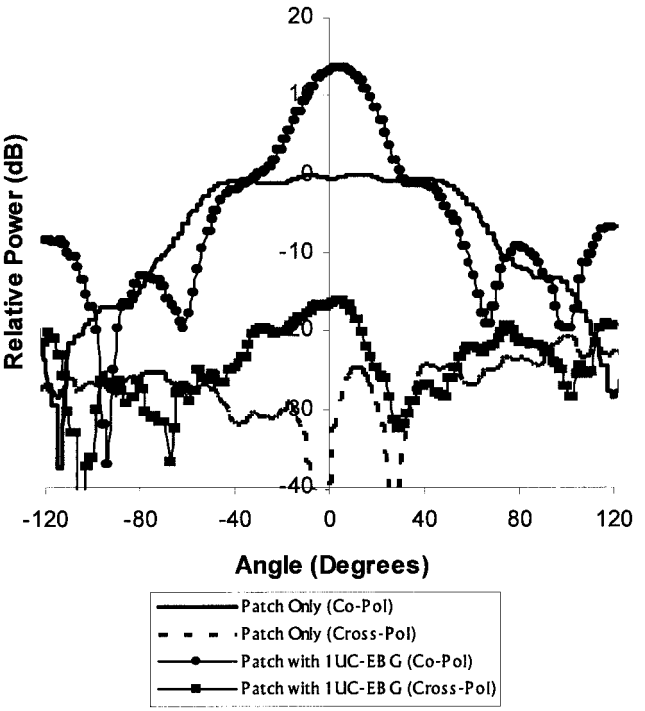

Figure 5 Comparison between the conventional patch and the antenna with 1 UC-EBG layer with measured E-field radiation pattern

UC-EBG cavities to a single-element patch antenna, instead of a conventional antenna-array system, numerical and experimental analyses were performed in order to validate the possibility of obtaining such characteristics. The cavity structure was numerically simulated with different positions and offset degrees of the patch antenna with regard to the UC-EBG layers. The produced pattern showed an asymmetric pattern with attenuation at certain directions more than others, as expected. Many measurements have been performed and they produced various patterns with different characteristics, but with the main beam direction not changing notably. Figure 7 shows the radiation pattern that results

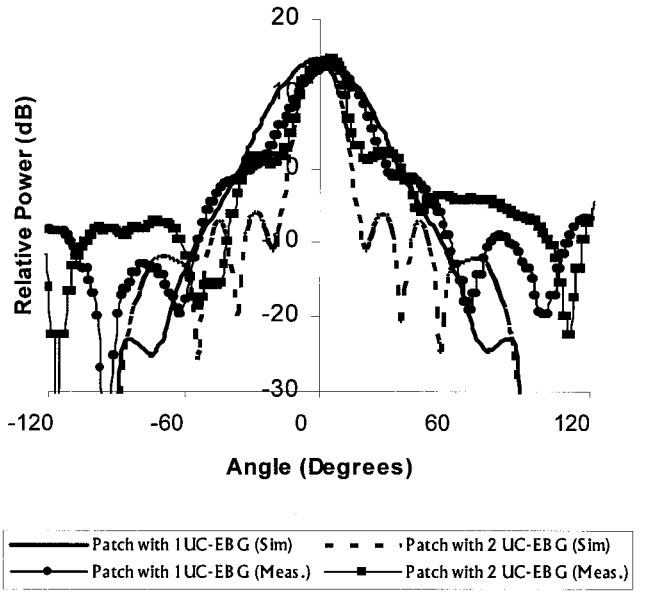

Figure 6 Radiation patterns of UC-EBG cavity antenna

from one of those measurements with an apparent variation in the attenuation level at both sides of the main beam. This was expected; because the patch antenna in the cavity is offset from the centre, its angular spectrum of radiation field will be alternated and becomes asymmetrical due to uneven attenuation from the EBG. Indeed, antenna-beam shaping can be further designated by changing EBG patterns.

The cavity structure studied here can be applied to different applications in the wireless-communication sector, such as wireless LAN and mobile-communication systems. Thus, it is interesting to study the behaviour of the antenna at different frequencies around the resonance and to obtain the bandwidth of the antenna. Figure 8 shows that the directivity keeps good values when the frequency is slightly shifted and the bandwidth is approximated to be around 2%, which illustrates the possibility of using such structure in the newly emerging WLAN application, HiperLAN (frequency range of 5.15 to 5.35 GHz).

In order to validate the practicality of the investigation and the structure presented in this paper, the measured radiation patterns of the shifted EBG structures for both one and two layers were compared to that produced by a nine-element antenna array, providing patterns desired in some mobile-service coverage applications. As shown in Figure 7, there is good agreement with slight differences in the existence of null points in the results obtained in this study. However, future work, including the design and study of various EBG structures and modelling techniques, will allow the introduction of fully configurable EBG structures and thus permit the forming of different patterns according to the applications in use.

5. CONCLUSION

A new application of the UC-EBG concept has been introduced, not only to improve directivity and gain of conventional patch antenna, but also to provide the feature of beam forming that is required in many current communication systems, such as Wireless LANs and mobile-communication systems. This paper has demonstrated that an antenna beam can be shaped by shifting the defects (patch antennas) from the centre of UC-EBG cavities. The size of the UC-EBG cavity can be further reduced by using high-permittivity dielectric materials. The experimental results show good agreement with the theoretical and numerical results. The concept presented here can be used as the basis for future work in developing simple, low-cost antenna systems to be implemented in many communication applications without the return to complicated array systems.

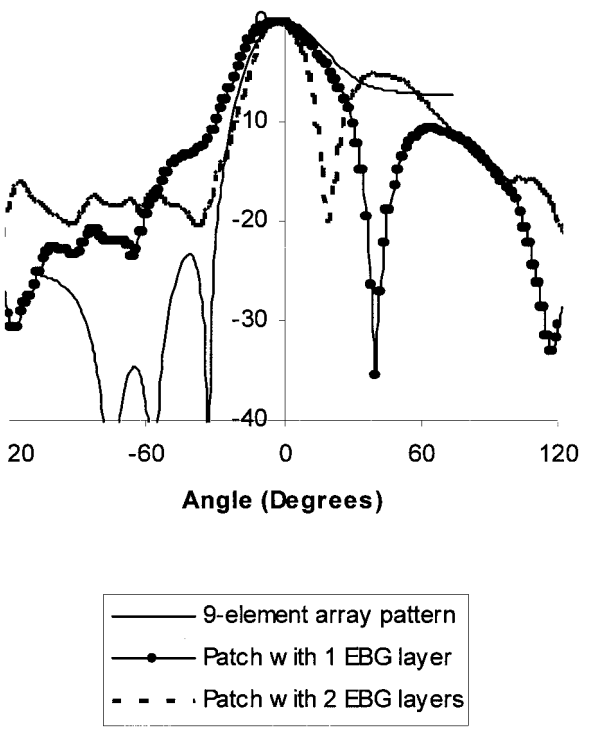

Figure 7 Comparison of beam-shaping patterns with that of a typical desirable mobile-service coverage pattern produced by a nine-element array

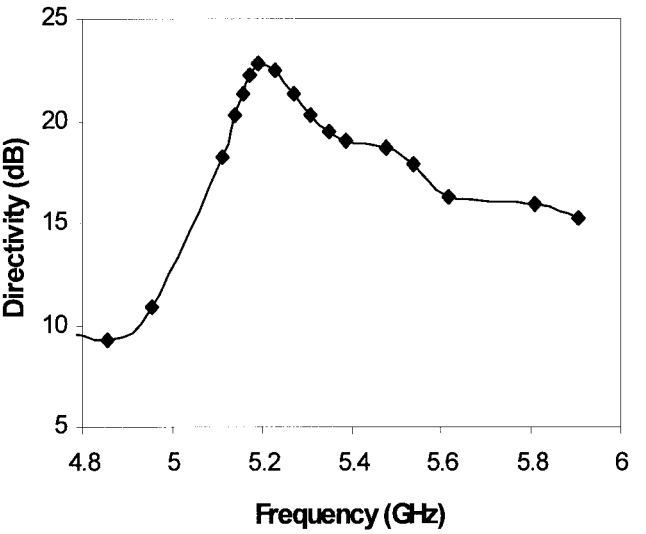

Figure 8 Simulated frequency response of the UC-EBG cavity antenna directivity with beam shaping

REFERENCES

1. E. Yablonovitch, Inhibited spontaneous emission in solid state physics and electronics, Phys Rev Lett 58 (1987), 2059–2062.
2. Y. Rahmat-Samii and H. Mosallaei, Electromagnetic bandgap structures: Classification, characterisation and applications, Proc. 11th Int Conf Antennas Propagat 2 (2001), 560–564.
3. Y. Hao and C.G. Parini, Microstrip antennas on various UC-PBG substrates, IEICE Trans Electron Special Issue Microwave and Millimeter-Wave Technol (2003).
4. R. Gonzalo, P. De Maagt, and M. Sorolla, Enhanced patch-antenna performance by suppressing surface waves using photonic-bandgap substrates, IEEE Trans Microwave Theory Tech 47 (1999), 2131–2138.
5. L. Zhan and Y. Rahmat Samii, PBG, PMC, and PEC ground planes: A case study of dipole antennas, IEEE Int Symp Antennas Propagat Salt Lake City, UT, 2000, pp. 674–677.
6. K.M. Shum, Q. Xue, C.H. Chan, and K.M. Luk, Gain enhancement of microstrip reflectarray incorporating a PBG structure, IEEE Int Symp Antennas Propagat Salt Lake City, UT, 2000, pp. 350–353.
7. T.-Y. Yun and K. Chang, A new PBG diplexer for a multi-band transceiver antenna system, IEEE Int Symp Antennas Propagat Boston, MA, 2001, pp. 490–493.
8. Y. Hao and C.G. Parini, Isolation enhancement of anisotropic UC-PBG microstrip diplexer patch antenna, IEEE Antennas Wireless Propagat Lett 1 (2002).
9. M. Thévenot, C. Cheype, A. Reineix, and B. Jecko, Directive photonic-bandgap antennas, Microwave Opt Technol Lett 47 (1999), 2115–2122.
10. T. Akalin, J. Danglot, O. Vanbesien, and D. Lippens, A highly direc-

tive dipole antenna embedded in a Fabry–Perot-type cavity, IEEE Microwave Wireless Compon Lett 12 (2002).
11. B. Temelkuran, E. Ozbay, J.P. Kavanaugh, G. Tuttle, and K.M. Ho, Resonant cavity enhanced detectors embedded in photonic crystals, Appl Phys Lett 72 (1998), 2376–2378.
12. G. Guida, D. Maystre, G. Tayeb, and P. Vincent, Electromagnetic modelling for three-dimensional metallic photonic crystals, J Electromagn Waves Applic 12 (1998), 1153–1179.
13. I. Abram, I. Robert, and R. Kuszelewicz, Spontaneous emission control in semiconductor microcavities with metallic or Bragg mirrors, IEEE J Quantum Electron 34 (1998), 71–76.
14. R. Sauleau, P. Coquet, T. Matsui, and Jean-Pierre Daniel, A new concept of focusing antennas using plane-parallel Fabry–Perot cavities with nonuniform mirrors, IEEE Trans Antennas Propagat 51 (2003), 3171–3175.
15. C. Caloz, C.C. Chang, and T. Itoh, A novel anisotropic uniplanar compact photonic band-gap (UC-PBG) ground plane, 31st Euro Microwave Conf, London, 2001, pp. 185–187.
16. R.H. Clarke and J. Brown, Diffraction theory and antennas, Ellis Horwood Ltd, London.
17. Y. Murakami, T. Kijima, H. Iwasaki, T. Ihara, T. Manabe, and K. Iigusa, A switchable multi-sector antenna for indoor wireless LAN systems in the 60-GHz band, IEEE Trans MTT 46 (1998), 841–843.

LOSSY TRANSMISSION LINE METAMATERIALS

Christophe Caloz and Tatsuo Itoh
Electrical Engineering Department
University of California
Los Angeles, CA 90095

Received 18 March 2004

ABSTRACT: *Lossy purely LH and generalized CRLH TL metamaterials are analyzed using both an ideal approach, assuming perfectly homogeneous media, and a lumped-element approach, taking into account the real periodic LC configuration of artificial metastructures. The effects of losses are identified and discussed. A CRLH TL metamaterial with small losses is shown to exhibit propagation characteristics identical to that of a lossless metamaterial.* © 2004 Wiley Periodicals, Inc. Microwave Opt Technol Lett 43: 112–114, 2004; Published online in Wiley InterScience (www.interscience.wiley.com). DOI 10.1002/mop.20392

Key words: *losses; metamaterials; left-handed (LH); composite right/left-handed (CRLH); transmission lines*

1. INTRODUCTION

Recently, left-handed (LH) metamaterials (materials with antiparallel phase and group velocities) [1] have received considerable attention [2]. Recognizing the importance of right-handed (RH) series-L/shunt-C parasitic contributions in a real LH TL metamaterial, essentially consisting of series-C/shunt-L, we have introduced the concept of composite right/left-handed (CRLH) metamaterials [3–5], which has proven adequate for the understanding and development of several novel microwave applications [6]. However, the effects of losses [7] in these TL structures have not been thoroughly studied so far. This is the object of the present contribution.

2. MODELS AND ANALYSIS OF TL METAMATERIALS

Figure 1 shows different models of lossy TL metamaterials. Figure 1(a) depicts a purely LH 1D TL, which is known to be unphysical

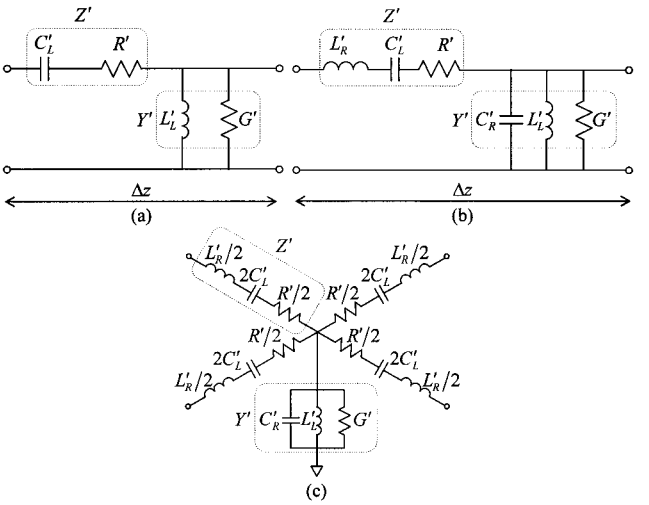

Figure 1 Different lossy TL metamaterial models: (a) purely LH TL; (b) CRLH TL; (c) generalization of (b) to 2D

(unbounded group velocity at high frequencies), but represents a good approximation of practical backward-wave structures at low frequencies [5]. The most general TL model in reality is the CRLH model, shown in Figure 1(b), where series-L and shunt-C parasitic effects have been included for accurate description of a practical "LH" structure, which supports backward waves only at low frequencies (LH range) and forward waves at high frequencies (RH range), with a gap or gapless transition between the two ranges, where the propagation constant β is zero. The conventional RH TL is obtained from the CRLH model by setting $L'_L = C'_L = 0$, while the purely LH TL of Figure 1(a) is the particular case where $L'_R = C'_R = 0$. Finally, the model of Figure 1(c) represents a 2D CRLH TL structure, which exhibits homogeneous (effective) and isotropic propagation characteristics (azimuthally symmetric), since the unit cell of a metamaterial is assumed to be electrically small, that is, $p \ll \lambda_g/4$, where λ_g is the guided wavelength and p is the average lattice constant of the structure, or its period if the structure is periodic.

CRLH TL metamaterials can be analyzed by two different approaches. Because $p \ll \lambda_g/4$, they are essentially equivalent to ideal/homogeneous TLs in their pass-band, and therefore their wavenumber $\gamma = \alpha + j\beta$ and characteristic impedance Z_0 are given by

$$\gamma = \sqrt{Z'Y'} = \sqrt{(R'G' - X'B') - j(R'B' + G'X')}, \quad (1)$$

$$Z_0 = \sqrt{\frac{Z'}{Y'}} = \sqrt{\frac{R' + jX'}{G' + jB'}} \overset{p/\lambda_g \to 0}{\approx} \sqrt{\frac{Z}{Y}} = \sqrt{\frac{R + jX}{G + jB}}, \quad (2)$$

with

$$Z' = R' + jX', \quad X' = \omega L'_R - 1/(\omega C'_L), \quad (3a)$$

$$Y' = G' + jB', \quad B' = \omega C'_R - 1/(\omega L'_L), \quad (3b)$$

where the per-unit and times-unit length parameters (primed expressions) are given and are related to the physical elements used to synthesize an artificial structure (nonprimed expressions) by